

Obtaining the Morse parameter for large bond-stretching using Murrell-Sorbie parameters

Teik-Cheng Lim

Received: 24 July 2007 / Accepted: 3 December 2007 / Published online: 21 December 2007
© Springer-Verlag 2007

Abstract Although the second derivative approach has been shown to provide good parameter relationships between any two interatomic potential functions, these relations are valid only at and near the equilibrium point. Arising from the significant discrepancy between connected potential functions for large stretching of covalent bonds by the second derivative approach, an integral approach is developed herein. By equating interatomic energy integral from equilibrium to bond dissociation, the overall discrepancy is minimized for that range between the Morse and Murrell-Sorbie potential functions. Plotted results reveal two observations. First of all, the second derivative approach is appropriate for bond compression and infinitesimal bond stretching, while the integral approach is more suitable when the extent of bond stretching is significant. Secondly, the Morse function exactly fits the Murrell-Sorbie curve when the Morse shape parameters based on the second derivative and integral approaches are equal. Hence a criterion for determining the accuracy level of Murrell-Sorbie parameters for conversion to Morse parameter is established. Finally, a demonstration was made for cases where a clear discrepancy was observed in the potential energy curves. It was found that the integral approach gives a more conservative and more realistic interatomic force curve than those of derivative approach.

Keywords Morse · Murrell-Sorbie · Parameter relations · Potential functions

T.-C. Lim (✉)
School of Science and Technology, SIM University (UniSIM),
535A Clementi Road,
S 599490 Singapore, Singapore
e-mail: alan_tc_lim@yahoo.com

Introduction

The importance of potential energy functions in molecular force fields is obvious - the accuracy of simulated results depends on the choice of these functions. Indeed, it has been reported that the use of different potential functions strongly influence the calculated size effects of nano-scale structures [1]. Although potential functions with greater number of parameters can be generally said to provide better fitting to experimental data than those of fewer parameters, the latter functions have been adopted to a greater extent in molecular mechanics softwares. For example, the Morse function

$$U_M = D \left(e^{-2\alpha(r-R)} - 2e^{-\alpha(r-R)} \right) \quad (1)$$

has been used for describing the energy of bond-stretching in the following force fields: CVFF [2], DREIDING [3], UFF [4] and ESFF [5]. Here, D is the magnitude of interatomic bond energy when the interatomic distance r is at the equilibrium bond length R , while α determines the shape of the potential energy curve. In addition, the Morse function has been used for quantifying the van der Waals interactions in the COSMIC force field [6]. Although the Rydberg potential function [7, 8]

$$U_{Ryd} = -D(1 + a\rho)e^{-a\rho}; \rho = \rho(R, r) \quad (2)$$

has three parameters like the Morse function, it has been expanded by Murrell et al. [9–11] into 5 parameters, i.e.

$$U_{MS} = -D(1 + a_1\rho + a_2\rho^2 + a_3\rho^3) \exp(-a_1\rho); \quad (3)$$
$$\rho = r - R$$

by expanding the original Rydberg function up to the third term, i.e. $a_3\rho^3$. In recent years, the Murrell-Sorbie potential

function has been extended up to the fourth terms for H_2 [12] and $HgZn$ [13], the eighth term for $SiCl^+$ [14], and even the ninth term for NaH [15]. In view of the greater number of parameters for the Murrell-Sorbie function, it can be said that this function allows a better fit to experimental data, thereby providing greater confidence when computing bond-stretching over large range. As such, the conversion of Murrell-Sorbie parameters, which are normally painstakingly obtained, into parameters of the Morse function, which is more widely incorporated in force fields, is justified for large bond stretching.

Analysis

Previous attempts in parameter conversion were focused on ensuring equal curvature at the minimum well-depths of the compared potential energy curves [16–21], thereby limiting the validity to very small change in the internuclear distance. In this paper, we replace the imposition of equal curvature with equal integral from equilibrium to dissociation. Figure 1 shows the similarity and dissimilarity between previous attempts and the proposed method.

Integral for the Morse function is easily obtained as

$$\int_0^\infty U_M d\rho = -\frac{3}{2} \left(\frac{D}{\alpha} \right). \quad (4)$$

Taking integration by parts for the Murrell-Sorbie function, we have

$$\int_0^\infty U_{MS} d\rho = -\frac{D}{a_1} - D \int_0^\infty (a_1 + 2a_2\rho + 3a_3\rho^2) \frac{\exp(-a_1\rho)}{a_1} d\rho \quad (5)$$

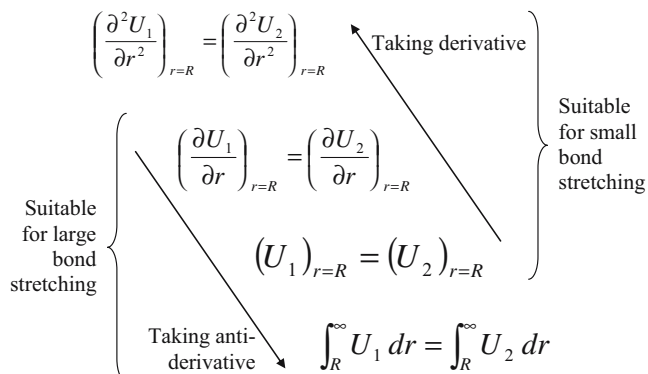


Fig. 1 Comparison between previous parameter conversion [16–21] suitable for small bond stretching and the present approach for large bond stretching

whereby

$$\int_0^\infty (a_1 + 2a_2\rho + 3a_3\rho^2) \frac{\exp(-a_1\rho)}{a_1} d\rho = \frac{1}{a_1} + \int_0^\infty (2a_2 + 6a_3\rho) \frac{\exp(-a_1\rho)}{a_1^2} d\rho \quad (6)$$

and

$$\int_0^\infty (2a_2 + 6a_3\rho) \frac{\exp(-a_1\rho)}{a_1^2} d\rho = \frac{2}{a_1^3} \left(a_2 + 3 \frac{a_3}{a_1} \right). \quad (7)$$

Substituting Eq. (7) into Eq. (6) which, in turn substituted into Eq. (5) gives

$$\int_0^\infty U_{MS} d\rho = -2 \left(1 + \frac{a_2}{a_1^2} + 3 \frac{a_3}{a_1^3} \right) \frac{D}{a_1}. \quad (8)$$

Comparing Eqs. (4) and (8) allows the Morse parameter to be expressed in terms of Murrell-Sorbie parameters as

$$\alpha = 0.75a_1 \left/ \left(1 + \frac{a_2}{a_1^2} + 3 \frac{a_3}{a_1^3} \right) \right. \quad (9)$$

To compare the present approach with the previous method, i.e. the second derivative approach, we let

$$\left(\frac{\partial^2 U_M}{\partial r^2} \right)_{r=R} = \left(\frac{\partial^2 U_{MS}}{\partial r^2} \right)_{r=R} \quad (10)$$

to give

$$\alpha = \sqrt{\frac{a_1^2 - 2a_2}{2}}. \quad (11)$$

Hence Eqs. (9) and (11) represent the conversion of Murrell-Sorbie parameters into the Morse parameter based on integral and second derivative approaches respectively.

Results and discussion

For comparison, we plot the Morse and Murrell-Sorbie potential energy functions in terms of non-dimensional bond-stretching energy (U/D) versus the change in bond length ($r-R$) based on the spectroscopic results of Huxley and Murrell [10]. From these Murrell-Sorbie parameters, the Morse parameter α was calculated based on Eqs. (9) and (11) and arranged in increasing difference between the values of α by both approaches. Three diatomic molecules were selected - FMg, FSi and FO - to represent two extreme cases and an almost overlapping case. Results of the calculated Morse parameters are listed in Table 1.

Figures 2–4 show the Murrell-Sorbie plots of FMg, FSi and FO diatomic molecules as circles with the Morse approximation represented as thin curves (integral approach) and thick curves (second derivative approach). Figure 2–4 are arranged in increasing magnitude of α , i.e.

Table 1 Extraction of Morse parameter from Murrell-Sorbie parameters

Diatoms	$a_1(\text{\AA}^{-1})$	$a_2(\text{\AA}^{-2})$	$a_3(\text{\AA}^{-3})$	$\alpha(\text{\AA}^{-1})$, Eq. (10)	$\alpha(\text{\AA}^{-1})$, Eq. (12)	Difference between both α
FMg	1.854	-0.341	0.854	1.067303	1.4352	-0.3678
MgO	1.909	-0.509	0.686	1.238378	1.5268	-0.2884
AlO	2.409	-0.418	1.106	1.550447	1.8220	-0.2715
MgS	1.780	-0.358	0.339	1.250777	1.3936	-0.1429
BF	3.200	1.930	2.926	1.647944	1.7861	-0.1381
AlF	2.479	1.172	1.484	1.253759	1.3787	-0.1249
BeO	2.828	0.477	1.029	1.773215	1.8766	-0.1034
CLi	1.700	0.533	0.496	0.857259	0.9550	-0.0977
FLi	2.196	1.102	1.151	1.059452	1.1442	-0.0848
FNa	2.006	0.987	0.957	0.93976	1.0124	-0.0727
BCl	2.457	1.067	1.012	1.333941	1.3969	-0.0630
CF	3.557	2.303	2.672	1.961379	2.0058	-0.0444
BeF	2.948	1.586	1.509	1.626704	1.6611	-0.0344
AlCl	2.150	1.052	0.824	1.092246	1.1222	-0.0299
FSi	3.008	1.807	1.605	1.63879	1.6483	-0.0096
BeS	2.128	-0.308	0.220	1.595242	1.6038	-0.0086
AlS	2.634	0.827	0.466	1.652172	1.6254	0.0268
OSi	3.208	1.685	1.217	1.888067	1.8603	0.0278
AlH	2.316	1.084	0.576	1.295115	1.2641	0.0310
MgMg	2.043	1.005	0.526	1.074629	1.0402	0.0345
CO	3.897	2.305	1.898	2.341966	2.2996	0.0423
ClNa	1.316	0.630	0.372	0.532525	0.4857	0.0468
BH	2.935	1.638	0.983	1.684469	1.6337	0.0507
HLi	2.173	1.088	0.447	1.197371	1.1283	0.0691
FH	4.216	3.965	3.835	2.296968	2.2186	0.0783
SSi	2.773	1.462	0.647	1.623338	1.5436	0.0797
HNa	2.154	1.071	0.365	1.205238	1.1175	0.0877
ClSi	2.880	2.021	1.140	1.557512	1.4581	0.0994
CS	3.445	2.370	1.238	2.002076	1.8879	0.1142
FP	3.521	2.863	1.835	1.945952	1.8264	0.1196
HH	3.961	4.064	3.574	2.075191	1.9444	0.1308
BeCl	3.100	2.475	1.417	1.660432	1.5264	0.1340
HSi	3.058	2.335	1.188	1.668817	1.5299	0.1389
CCl	3.463	2.360	1.000	2.046643	1.9069	0.1398
BN	4.487	5.580	6.391	2.259479	2.1182	0.1413
LiNa	1.846	0.993	0.237	0.985814	0.8431	0.1427
HS	3.284	1.837	0.494	2.031878	1.8856	0.1463
CH	3.836	3.511	2.268	2.116778	1.9612	0.1555
BS	3.526	2.768	1.327	2.013397	1.8570	0.1564
NSi	3.732	2.975	1.460	2.156616	1.9972	0.1594
LiLi	1.919	1.077	0.232	1.034726	0.8742	0.1605
ClH	3.698	3.349	1.999	2.034131	1.8678	0.1664
SiSi	2.957	2.300	0.962	1.613306	1.4394	0.1739
BO	4.253	3.967	2.368	2.431838	2.2532	0.1786
HO	4.507	4.884	3.795	2.476748	2.2962	0.1806
NaNa	2.067	1.384	0.365	1.07067	0.8673	0.2034
OP	4.275	4.399	2.717	2.383773	2.1769	0.2069
HP	3.645	3.470	1.771	1.994147	1.7813	0.2129
BB	3.581	2.787	0.752	2.120672	1.9039	0.2168
HN	4.482	4.971	3.397	2.470519	2.2524	0.2182
AlAl	2.634	1.536	0.038	1.609199	1.3903	0.2189
SS	3.954	4.312	2.332	2.135021	1.8722	0.2628
PP	3.920	4.266	2.246	2.115902	1.8486	0.2673
NP	4.491	5.165	2.882	2.492162	2.2180	0.2742
FN	4.895	6.571	5.197	2.608969	2.3258	0.2831
CIF	4.137	3.311	0.213	2.580285	2.2905	0.2898

Table 1 (continued)

Diatoms	$a_1(\text{\AA}^{-1})$	$a_2(\text{\AA}^{-2})$	$a_3(\text{\AA}^{-3})$	$\alpha(\text{\AA}^{-1})$, Eq. (10)	$\alpha(\text{\AA}^{-1})$, Eq. (12)	Difference between both α
NO	5.398	7.041	4.823	3.0357	2.7438	0.2919
OS	4.748	6.504	5.228	2.481467	2.1835	0.2979
CP	4.487	5.506	3.156	2.44162	2.1356	0.3061
NN	5.396	7.328	4.988	3.004636	2.6889	0.3157
HMg	3.815	4.499	2.455	1.984548	1.6668	0.3178
NS	4.926	6.677	4.539	2.659666	2.3358	0.3239
CC	5.026	6.630	3.787	2.788199	2.4496	0.3386
CN	5.312	7.663	5.369	2.888989	2.5388	0.3502
CICl	4.478	6.022	3.749	2.35591	2.0011	0.3548
BeH	4.278	5.873	3.858	2.184532	1.8104	0.3741
CIO	5.142	7.971	6.116	2.684782	2.2911	0.3937
FS	5.040	7.564	5.072	2.668306	2.2665	0.4019
FF	6.538	12.521	11.717	3.456339	2.9752	0.4812
OO	6.080	11.477	11.003	3.128994	2.6469	0.4821
FO	7.228	18.759	22.835	3.519038	2.7135	0.8056

the curvature at the minimum well-depth. For the purpose of comparison, these three figures were plotted in the same scale, i.e. $-1 \leq (U/D) \leq 0.4$ and $-0.5\text{\AA} \leq r - R \leq 2.5\text{\AA}$.

In Fig. 2, the Morse parameter α by integral approach is smaller than that by second derivative. As a result, the Morse function via second derivative (thick curve) agrees well with the Murrell-Sorbie curve for bond compression and very small bond stretching. At larger bond stretching, this Morse curve overestimates the Murrell-Sorbie curve. The smaller curvature at the minimum well-depth of the Morse curve via the integral approach gives underestimated bond energy for bond compression and small bond stretching. Due to the larger inflexion slope for the Morse function in the case of FMg, the Morse curve with its

parameter obtained by integral approach increases in such a manner that it crosses the Murrell-Sorbie curve, thereby providing lower error compared to the Morse curve with its parameter obtained by second derivative.

Not surprisingly, the Morse curves whereby the parameters were obtained by integral and second derivative approaches overlap for the case of FSi diatom, as shown in Fig. 3. This observation can be attributed to the almost equal Morse parameter by either approach. In addition, these two overlapping Morse curves exhibit very good agreement with the Murrell-Sorbie curve.

Figure 4 for FO diatom represents a case which is opposite to Fig. 2 in that the Morse parameter by integral approach is greater than that by second derivative. Like Fig. 2 for FMg, Fig. 4 shows good agreement between the

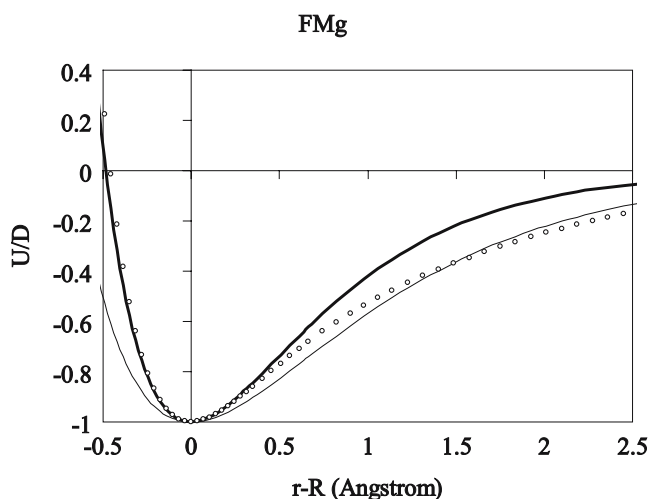


Fig. 2 Non-dimensionalized FMg stretching energy using Murrell-Sorbie function (circles) and the converted Morse curves based on integral approach (thin curve) and second derivative approach (thick curve)

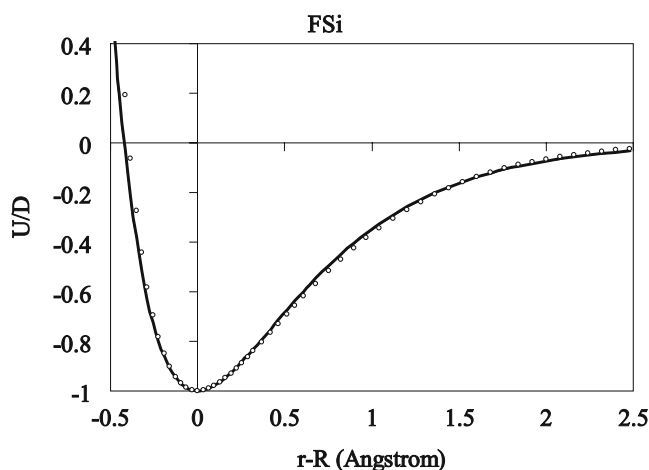


Fig. 3 Non-dimensionalized FSi stretching energy using Murrell-Sorbie function (circles) and the converted Morse curves based on integral approach (thin curve) and second derivative approach (thick curve)

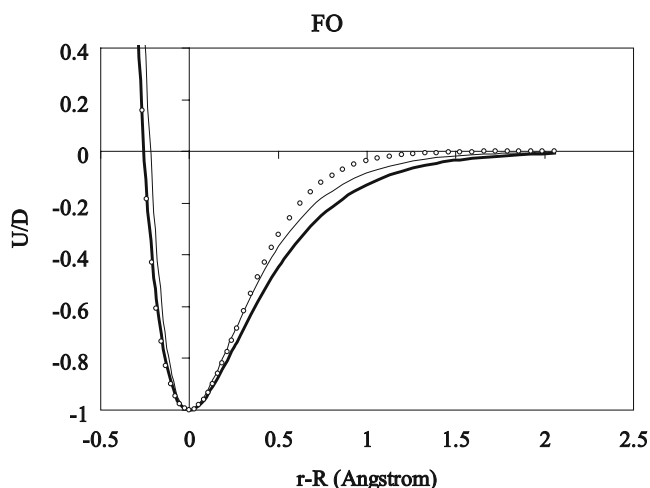


Fig. 4 Non-dimensionalized FO stretching energy using Murrell-Sorbie function (circles) and the converted Morse curves based on integral approach (thin curve) and second derivative approach (thick curve)

Murrell-Sorbie and the Morse approximation via second derivative approach (thick curve) for bond compression and at the vicinity of the minimum well-depth. Thereafter, the Morse approximation with its parameter obtained via integral (thin curve) exhibits closer agreement to the Murrell-Sorbie curve. Unlike Fig. 2, the Morse curve corresponding to its parameter by integral approach gives higher energy value than that of small stretching. This is attributed to the larger α by Eq. (9) than Eq. (11) for the case of FO diatom.

It is observed that when the Morse parameter α by the integral and second derivative approaches are equal, or almost equal, by Eqs. (9) and (11), then the Morse curve gives an almost exact agreement with the Murrell-Sorbie curve throughout the entire change in bond length, be it bond compression, large bond stretching or near the

minimum well-depth (see Fig. 3). In other words, the criterion for good Murrell-Sorbie to Morse parameter conversion is determined by the following condition:

$$0.75a_1 / \left(1 + \frac{a_2}{a_1^2} + 3 \frac{a_3}{a_1^3} \right) \cong \sqrt{\frac{a_1^2 - 2a_2}{2}} \tag{12}$$

and, whereupon this condition is fulfilled, either Eqs. (9) and (11) would give a good Morse parameter that enables its function to satisfactorily overlap with the Murrell-Sorbie potential energy curve. This criterion can be explained as follows. Equation (9) ensures zero overall error for both the functions' integral from $r=R$ to $r \rightarrow \infty$ in such a manner that the Morse curve crosses the Murrell-Sorbie function, but leaving the curvatures of both functions at the equilibrium point compromised - i.e. not equal. Equation (11) ensures equal curvatures of both curves at $r=R$ without considering the overall discrepancies at larger bond stretching. When both Eqs. (9) and (11) give equal value, we have equal minimum well-depth curvatures as well as equal slope at the crossing point - thereby ensuring conformity of the Morse function on the Murrell-Sorbie curve over the entire range of the stretched bond length.

Previous adjustments of the Morse parameter α resulted in an unwelcome change of the interrelated well depth D or even the equilibrium bond length R , as reviewed by Gardner and von Szentpaly [22, 23]. However, this change does not appear due to the non-dimensionalized working in terms of U/D and r/R . However, it should be mentioned here that the important scaling property of the original Morse curve is lost by its reparametrization via the present integral and second derivative approaches.

The validity of the newly proposed method for converting Murrell-Sorbie parameters into Morse parameter, within the context of interatomic energy, has been shown in

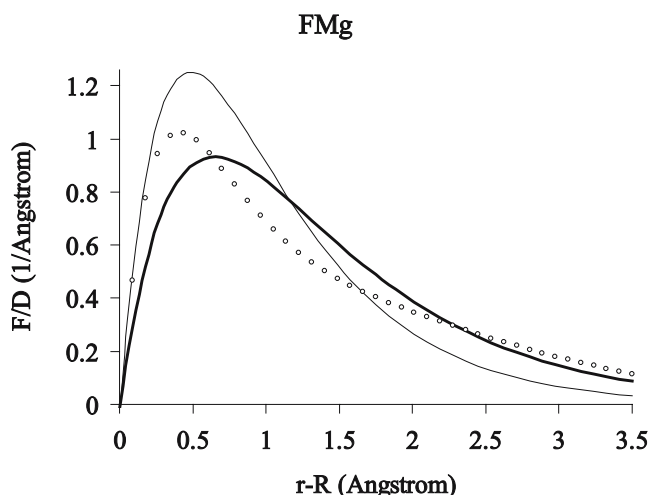


Fig. 5 Interatomic stretching force of FMg according to Murrell-Sorbie (circles) and the converted Morse curves based on second derivative (thin curve) and integral (bold curve) approaches

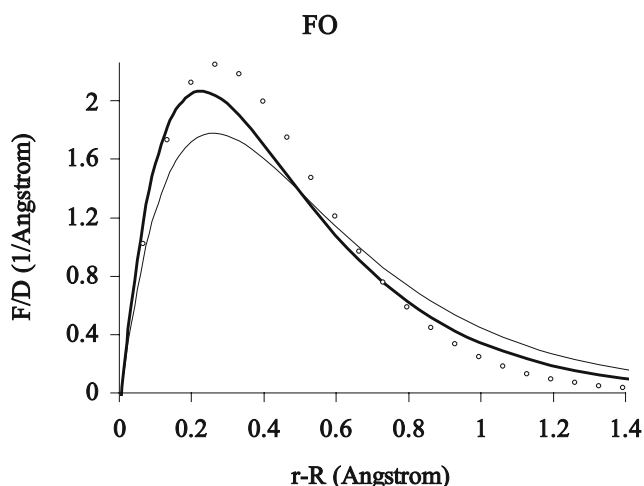


Fig. 6 Interatomic stretching force of FO according to Murrell-Sorbie (circles) and the converted Morse curves based on second derivative (thin curve) and integral (bold curve) approaches

Figs. 2–4. To show the impact on molecular dynamics calculation, we plot the interatomic force versus the change in bond length. Since both the Morse curves by second derivative and integral approaches strongly correlate with the Murrell-Sorbie curve for the FSi diatomic molecule (Fig. 3), we herein plot the (F/D) versus $(r-R)$ curves for FMg and FO diatoms. See also the graphical abstract.

Figure 5 shows the Murrell-Sorbie curve of FMg. The second derivative approach gives equal slope at $r=R$ but overestimates the force by which the bond experiences instability. The integral approach gives a lower instability force. Hence the integral approach gives a conservative result while the derivative approach gives a less reliable result.

The Murrell-Sorbie curve of FO is shown in Fig. 6. The second derivative approach gives an overly conservative instability force. Although the integral approach also underestimates the instability force, it gives a more realistic agreement with the Murrell-Sorbie curve, as demonstrated by its better proximity to the Murrell-Sorbie curve.

Conclusions

An expression for the Morse parameter in terms of Murrell-Sorbie parameters has been obtained for enabling a Morse function to be plotted with minimal error with respect to the Murrell-Sorbie curve for the case of large bond stretching. This was achieved by equating integrals of both functions from equilibrium bond length to bond dissociation. A comparison was made with the Morse curve whose parameter was obtained by equating the curvatures of both functions at the equilibrium bond length. Two observations were made. Where the Morse parameters vary significantly, the one based on equal curvature at equilibrium gives good agreement with the Murrell-Sorbie curve near the equilibrium and for bond compression, while the Morse parameter based on equated integral gives better approximation for large bond stretching. Secondly, the Morse function fits the Murrell-Sorbie curve perfectly when the Morse parameter by second derivative and integral approaches are equal. This second observation establishes a very important

criterion by which the suitability of Murrell-Sorbie parameters for conversion into Morse parameters is assessed. The conversion of a highly flexible potential such as the Murrell-Sorbie function to a simpler potential such as the Morse function essentially enables a commonly used potential function to be executed using highly accurate parameters.

References

1. Xiao SP, Hou WY (2006) Fullerenes Nanotubes Carbon Nanostruct 14:9–16
2. Lifson S, Hagler AT, Dauber P (1979) J Am Chem Soc 101:5111–5121
3. Mayo SL, Olafson BD, Goddard WA (1990) J Phys Chem 94:8897–8909
4. Rappe AK, Casewitt CJ, Colwell KS, Goddard WA, Skiff WM (1992) J Am Chem Soc 114:10024–10035
5. Barlow S, Rohl AA, Shi S, Freeman CM, O'Hare D (1996) J Am Chem Soc 118:7578–7592
6. Morley SD, Abraham RJ, Haworth IS, Jackson DE, Saunders MR, Vinter JG (1991) J Computer-Aided Mol Des 5:475–504
7. Rydberg R (1931) Z Physik 73:376–385
8. Rydberg R (1933) Z Physik 80:514–524
9. Murrell JN, Sorbie KS (1974) J Chem Soc Faraday Trans II 70:1552–1557
10. Huxley P, Murrell JN (1983) J Chem Soc Faraday Trans II 79:323–328
11. Murrell JN, Carter S, Farantos SC, Huxley P, Varandas AJC (1984) Molecular potential energy functions. Wiley, New York
12. Yang CL, Huang YJ, Zhang X, Han KL (2003) J Mol Struct (Theochem) 625:289–293
13. Gao F, Yang CL, Ren TQ (2006) J Mol Struct (Theochem) 758:81–85
14. Ren TQ, Ding SL, Yang CL (2005) J Mol Struct (Theochem) 728:159–166
15. Yang CL, Zhang X, Han KL (2004) J Mol Struct (Theochem) 676:209–213
16. Lim TC (2003) Z Naturforschung A 58:615–617
17. Lim TC (2004) Phys Scripta 70:347–348
18. Lim TC (2005) Chem Phys 320:54–58
19. Lim TC (2006) Mol Phys 104:1827–1831
20. Lim TC (2007) J Math Chem 41:135–142
21. Lim TC (2007) Chem Phys 331:270–274
22. Gardner DON, von Szentpaly L (1999) J Phys Chem A 103:9313–9322
23. Gardner DON, von Szentpaly L (2001) J Phys Chem A 105:9467–9477